Phytomedicine 20 (2013) 890–896

Contents lists available at SciVerse ScienceDirect

Phytomedicine

journal homepage: www.elsevier.de/phymed

Preparation of novel antiproliferative emodin derivatives and studies on their cell cycle arrest, caspase dependent apoptosis and DNA binding interaction☆

T. Narender[a,*], P. Sukanya[a], Komal Sharma[b], Surendar Reddy Bathula[b,*]

[a] Medicinal and Process Chemistry Division, CSIR-Central Drug Research Institute, Lucknow 226 001, UP, India
[b] Pharmaceutics Division, CSIR-Central Drug Research Institute, Lucknow 226 001, UP, India

ARTICLE INFO

Keywords:
Emodin derivatives
Rheum emodi
Anticancer agents
Anthraquinones
Apoptosis
Caspase-3
Cell cycle

ABSTRACT

Emodin (**1**) is the major bioactive compound of several herb species, which belongs to anthraquinone class of compound. As a part of our drug discovery program, large quantities of emodin (**1**) was isolated from the roots of *Rheum emodi* and a library of novel emodin derivatives **2**–**15** were prepared to evaluate their antiproliferative activities against HepG2, MDA-MB-231 and NIH/3T3 cells lines. The derivatives **3** and **12** strongly inhibited the proliferation of HepG2 and MDA-MB-231 cancer cell line with an IC_{50} of 5.6, 13.03 and 10.44, 5.027, respectively, which is comparable to marketed drug epirubicin (**III**). The compounds **3** and **12** were also capable of inducing cell cycle arrest and caspase dependent apoptosis in HepG2 cell lines and exhibit DNA intercalating activity. These emodin derivatives hold promise for developing safer alternatives to the marketed epirubicin.

Introduction

Anthraquinones are widely distributed secondary metabolites of plants (aloe, cascara sagrada, senna and rhubarb), microbes, lichens and insects, which possess various biological activities (Zaprometnov 1993; Gorelik 1983; Fain 1999). Anthraquinones isolated from the microbes such as daunorubicin (**I**), doxorubicin (**II**), epirubicin (**III**) and several synthetic analogs such as mitoxantrone (**IV**) and pixantrone (**V**) are in clinical use for the treatment of various cancers (Fig. 1). Emodin (**1**) belongs to anthraquinone class of compound is the major bioactive compounds of numerous herb species such as *Rheum*, *Polygonum* (polygonaceae), *Rhamnus* (Rhamnaceae) and *Cassieae* (senna) (Alves et al. 2004; Liang et al. 1993; Yang et al. 1999) and possesses immunosuppressive, anticancer, anti-inflammatory, anti-atherosclerotic, and vasorelaxant effects (Kuo et al. 2001; Huang et al. 1991; Zhou and Chen 1998; Koyama et al. 1988). Several reports have shown that emodin (**1**) has antiproliferative effects on many kinds of cancer cell lines such as HER-2/neu over expressing breast cancer (Zhang et al. 1998, 1999), leukemia (Chun et al. 2010; Chen et al. 2002), hepatoma (Shieh et al. 2004) and lung (Su et al. 2005) cancer cells. Also, emodin-triggered apoptosis is mediated through the caspase and mitochondria dependent pathways in proximal tubular epithelial HK-2 cells (Wang et al. 2007). Emodin enhanced gefitinib induced cytotoxicity via Rad51 down regulation and ERK1/2 inactivation in human breast cancer BCap-37 cells (Chen et al. 2009).

As a part of our drug discovery program on anticancer agents from Indian medicinal plants, we isolated large quantities of emodin (**1**) from the roots of *Rheum emodi* and planned to carry out chemical transformation to improve its therapeutic application. Chemical transformation of bioactive compounds of medicinal herbs is one of the most common approaches in drug discovery to improve the therapeutic properties. For example the anticancer drugs teniposide and etoposide are derivatives of podophyllotoxin and topotecan and irinotecan are analogs of camptothecin, which have better therapeutic benefits than the parent natural products.

Materials and methods

General chemistry

IR spectra were recorded on Perkin-Elmer RX-1 spectrometer. Using either KBr pellets (or) in neat. ^{1}H NMR, ^{13}C NMR, DEPT-90 and DEPT-135 spectra were run on Bruker Advance DPX 300 MHz and 200 MHz in $CDCl_3$.Chemical shifts are reported as values in ppm relative to $CHCl_3$ (7.26) in $CDCl_3$ and TMS was used as internal standard. ESI mass spectra were recorded on JEOL SX 102/DA-6000. Chromatography was executed with silica gel (60–120 mesh) using mixtures of chloroform, ethyl acetate and hexane as eluants.

Background of plant

R. emodi wall. (Family: Polygonaceae, commonly known as revand-chini and English name rhubarb) is a stout herb, distributed

☆ This is CDRI communication No. 8449.

* Corresponding authors. Tel.: +91 522 2612411; fax: +91 522 2623405.
E-mail addresses: t_narendra@cdri.res.in, tnarender@rediffmail.com (T. Narender), bsreddy@cdri.res.in (S.R. Bathula).

0944-7113/$ – see front matter © 2013 Elsevier GmbH. All rights reserved.
http://dx.doi.org/10.1016/j.phymed.2013.03.015

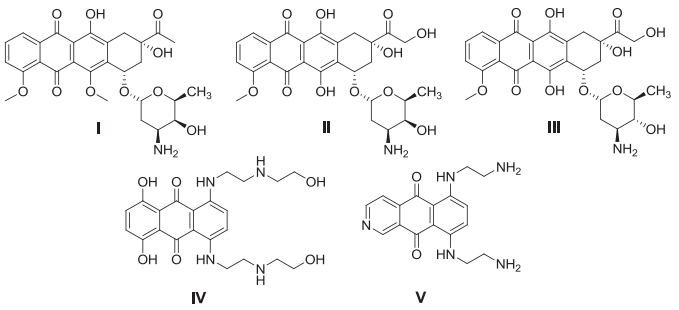

Fig. 1. Anticancer drugs with anthraquinone skeleton: daunorubicin (**I**), doxorubicin (**II**), epirubicin (**III**) mitoxantrone (**IV**), and pixantrone (**V**).

in the alpine and sub-alpine zones of the Himalayas (Agarwal et al. 2000; Singh et al. 2005). The roots of this species are used widely in ayurvedic medicine. Roots of the Indian rhubarb is darker, inferior in aroma, is a well known stomachic, bitter, cathartic and used all over the world.

Collection of medicinal plant

R. emodi wall. (Bark) was collected from India and the authentification was done by Botany Division of Central Drug Research Institute, Lucknow and kept in the herbarium for future reference.

Extraction

Powdered *R. emodi* wall. (Bark) (3 kg) were placed in glass percolator with 95% ethanol (10.l) and allowed to stand for 24 h at room temperature. The percolate was collected and these processes were repeated for four times. The combined percolate was evaporated under reduced pressure at 50 °C to afford ethanol extract. The weight of extract was found to be 200 g.

Isolation and purification of anthraquinone

The alcoholic extract was (200 g) chromatographed on a column of silica gel (60–120 mesh), eluted with Hexane and chloroform (70:30); recrystallization from methanol afford emodin (3 g). The compound visualization was obtained under UV light, also shown orange spot by spraying with 10% sulphuric acid in methanol.

Preparation of emodin derivatives

General method for O-alkylation (method A)

To a magnetically stirred solution of compound (100 mg, 0.00037 moles) in DMF (5 ml) at room temperature was treated with the respective aliphatic halo long chain (RX) (0.00033 moles) and K_2CO_3 (0.00092 moles). The whole reaction mixture was stirred for 4 h at 60–70 °C. It was then extracted with ethyl acetate (3 × 25 ml), the organic layer was washed with water, dried over anhyd Na_2SO_4 and evaporated under reduced pressure. Then the crude product was chromatographed on silica gel to afford the desired compound.

General method for C-alkylation (method B)

To a magnetically stirred solution of amine (0.0022 moles) cooled at 0 °C was slowly treated with formalin (0.00148 moles), glacial acetic acid (0.0192 moles) and compound **1** (100 mg, 0.00037 moles). The whole reaction mixture was brought to RT and stirred for 4 h, after pH was adjusted to 8 by addition of 20% aq. NaOH. It was then extracted with ethyl acetate (3 × 25 ml), the organic layer was washed with water, dried over anhyd. Na_2SO_4 and evaporated under reduced pressure. Then the crude product was chromatographed on silica gel to afford the desired compound.

General method for esterification and acid formation (method C)

Compound **1** (100 mg, 0.00037 moles) magnetically stirred in a solution of pyridine (2 ml) and acetic anhydride (0.00185 moles) at 60–70 °C for 4 h. The reaction mixture was put into cold water for crystallization, then filtered and dried. To the resultant crude acetate was gradually added 10 ml of acetic anhydride and glacial acetic acid mixture (1:1) and CrO_3 at 45 °C and stirred for 10 h at 70 °C. Acetic anhydride and glacial acetic acid mixture was removed by vacuum. It was then extracted with ethyl acetate (3 × 25 ml), the organic layer was washed with water, dried over anhyd Na_2SO_4 and evaporated under reduced pressure. Then the crude product was chromatographed on silica gel to afford the desired compound.

Biological study

Materials

MDA-MB-231, HepG2, and NIH/3T3 cell lines used in the present study was obtained from ATCC (American Type Culture Collection, USA). Annexin V FITC Apoptosis Detection Kit, MTT dye and Caspase-3 Activation Kit was procured from Sigma–Aldrich. Absorbance was recorded using Eliza Plate Reader. Flow cytometry was performed using a FACScan (Becton Dickinson, Mountain View, CA) flowcytometer.

Cell culture

MDA-MB-231 cells were routinely maintained in Dulbecco's Modified Eagle Medium DMEM (Sigma–Aldrich) while HepG2, NIH/3T3 cells were maintained in Roswell Park Memorial Institute (RPMI 1640, Merck) supplemented with 10% FBS (Merck) and 1% Antibiotic-Antimycotic Solution (Merck) at 37 °C in a humidified incubator with 5% CO_2. All stock solution of solutions of the compound were prepared in cell culture grade DMSO and stored in −20 °C. Compounds were diluted in culture media prior to use in experiments.

Cell viability assay

Antiproliferative activity of the compounds was tested by the 3-(4,5-dimethylthiazol-2-yl)-2,5-diphenyl tetrazolium bromide (MTT) assay. Briefly, cells (4×10^3 cells/well) were cultured in 96 well tissue culture plates and treated with different concentrations of compounds for 48 h. At the end of incubations, 10 μl of MTT (10 mg/ml) was added to the wells and incubated for 3 h. Absorbance was recorded at 540 nm using Eliza Plate Reader. All the experiments were repeated at least thrice independently. Values are expressed as mean ± SEM.

Apoptosis studies

Quantitation of apoptotic cells by Annexin V staining was carried out according to the manufacturer's instructions (Calbiochem). Briefly, HepG2 cells (5×10^5 cells/well) were seeded in 6 well plates and treated with 5, 10 and 20 μM of compound **3** and **12** and staurosporine (1 μg/ml) as positive control for 24 h. After the incubations, cells prepared as a suspension in 500 μl of cold PBS, centrifuged for 5 min at 1000 × *g* then resuspended in 500 μl cold 1× binding buffer and added 1.25 μl of Annexin V FITC and incubated for 15 min at RT in dark, centrifuge at 1000 × *g* for 5 min at RT, remove supernatant, gently resuspend in 500 μl cold 1× binding buffer and added 10 μl PI. Flow cytometry was performed using a FACScan (Becton Dickinson, Mountain View, CA) flowcytometer, equipped with a single 488-nm argon laser. Annexin V-FITC were analyzed using excitation and emission settings of 488 nm and 535 nm (FL-1 channel); PI, 488 nm and 610 nm (FL-2 channel). Debris and clumps were gated out using forward and orthogonal

light scatter. The experiment was repeated three times independently.

Cell cycle analysis

For cell cycle distribution studies post-treatment, cells were fixed in 70% ethanol, rehydrated in PBS with ribonuclease A (100 μg/ml) and Triton-X (10 μg/ml) for 30 min at room temperature then added PI (50 μg/ml) and incubated in dark for 30 min and analyzed with FACScan flow cytometer (Becton Dickinson, Mountain View, CA) equipped with an argon laser to give 488 nm light.

Caspase-3 activation assay

The activity of caspase-3 was determined using caspase-3 colorimetric assay kit (Sigma–Aldrich) according to the manufacturer's protocol. Briefly, HepG2 cells and NIH/3T3 cells (1 x 10^6cells/well) were treated with 0 μM, 10 μM and 20 μM compounds **3** and **12** for 24 h. The cells were harvested and lysed by addition of lysis buffer. Samples of the cell lysates were mixed with colorimetric substrate (Ac-DEVD-pNA) and incubated at 37 °C in the dark for 4 h. The absorbance was measured at 405 nm in an ELISA reader. Caspase-3 activity was expressed as the change of the activity compared to the control.

DNA intercalation assay

Calf thymus DNA (8.8 μM) was loaded with Tris buffer containing ethidium bromide (4.4 μM). To each well were added compounds **3**, **12**, and DOX at 5, 10 and 20 μM. After incubation for 30 min at 25 °C fluorescence was measured by using fluorimeter in duplicate experiments with two control wells (no compound = 100% fluorescence and no DNA = 0% fluorescence). Fluorescence readings are reported as % fluorescence readings compared to controls.

Statistical analysis

Each experiment was observed in triplicate. The data are presented as mean ± SD and compared using Student's *t*-test. $P < 0.05$ or less was considered to be statistically significant.

Results and discussion

Chemistry

We here report the synthesis of novel O-alkylated derivatives **2**–**6** (Fig. 2), C-alkylated derivatives **7**–**12** (Fig. 3), acyl derivatives **13**–**14** (Fig. 4) and acid derivative **15** (Fig. 4) from **1** and their anticancer profile against human hepatocellular carcinoma (HepG2), metastatic human breast cancer (MDA-MB-231) and embryonic fibroblast (NIH/3T3) cells lines. **3** and **12** showed comparable in vitro anticancer activity with marketed drug epirubicin **III** (Fig. 1 and Table 1), therefore **3** and **12** were selected for apoptosis inducing ability by flow cytometry, caspase-3 activity in HepG2 cells, HepG2 cells on cell cycle distribution studies and DNA binding interaction.

In order to prepare O-alkylated derivatives (**2**–**6**), hydroxyl group at meta position of emodin (**1**) was alkylated with various amine side chains under basic conditions using K_2CO_3 and DMF as a solvent.

To study the substituent effect on anthraquinone nucleus C-alkylated derivates **7**–**12** were prepared using Mannich reaction protocol (Kemertelidze and Gotsiridze 1971a,b; Blicke 1942; Brewster and Eliel 1953; Kintsurashvili et al. 1999).

Since the emodin (**1**) contain free hydroxyl group we planned to prepare few esters to study their anticancer activity. To prepare ester derivative **13** and **14**, emodin (**1**) was reacted with tiglic

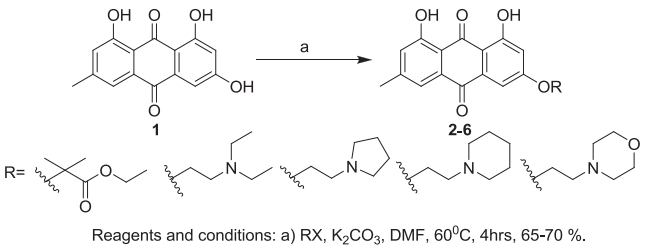

Fig. 2. Preparation of O-alkylated derivatives **2**–**6** of emodin (**1**).

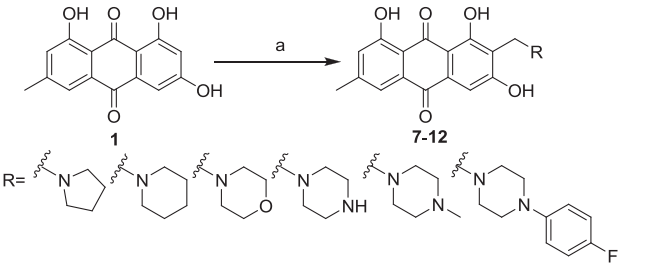

Fig. 3. Preparation of C-alkylated derivatives **7**–**12** of emodin (**1**).

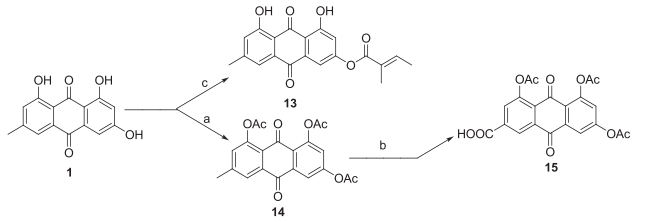

Fig. 4. Preparation of ester derivatives **13**, **14** and acid (**15**) from emodin (**1**).

acid in presence of triethylamine at 0 °C and acetic anhydride in presence of pyridine respectively (Fig. 4). To transform the methyl group in to acid functionality, emodin triacetate (**14**) was oxidized with chromium trioxide in presence of glacial acetic acid and acetic anhydride to provide acid (**15**) (Rahimipour et al. 2001).

Biological evaluation

Antiproliferative activity

All the compounds were screened against two cancer cell lines (HepG2 and MDA-MB-231) and a non-cancer cell line (NIH/3T3). The parent compound, emodin (**1**) has an IC_{50} of 291 μM, 119 μM and 212 μM against MDA-MB-231, HepG2 and NIH/3T3 respectively (Table 1). All the derivatives **2**–**15** prepared from emodin (**1**) have exhibited improved in vitro anticancer activity against MDA-MB-231 cell lines with better therapeutic index (Table 1). Except **7**, **8**, and **13**–**15** all other derivatives have also exhibited improved activity against HepG2 cell lines. Derivatives **2** (IC_{50} = 7.7 μM), **6** (IC_{50} = 4.2 μM), and **12** (IC_{50} = 5.0 μM) have IC_{50} below 10 μM against MDA-MB-231 cell lines, where as derivatives **3** (IC_{50} = 5.64 μM) and **12** (IC_{50} = 10.4 μM) also have IC_{50} of 10 μM or below 10 μM against HepG2 cell line. Our structure activity relationships indicated that O-alkylation and C-alkylation of emodin (**1**) improves the activity in both cell lines, where as esterification only improves the activity in MDA-MB-231 cell line. O-alkylated derivative **3** found to be 21-fold more potent in HepG2 cell line and 22-fold more potent in MDA-MB-231 cell

Table 1
Chemical structures and in vitro anticancer activity (IC_{50} in μM) of emodin (**1**) and its derivatives (**2**–**15**).

Comp. no	Chemical structure	IC_{50}(μM)		
		HepG2	MDA-MB-231	NIH/3T3
1	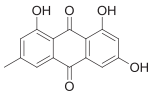	119	291	212
2	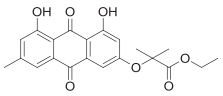	54.49	7.72	17.86
3	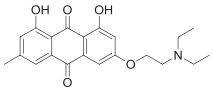	5.64	13.03	11.61
4	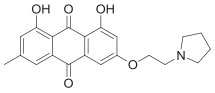	63.19	22.14	145
5	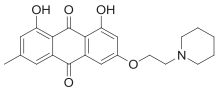	23.15	35	29.98
6	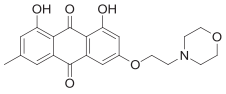	27	4.24	40.99
7	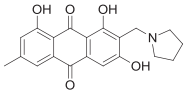	348	73.3	340
8	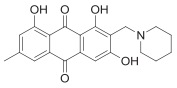	122	12.29	122
9	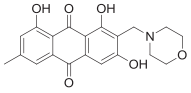	17.88	29.16	17.82
10	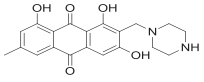	63	41.16	112
11	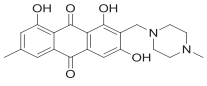	62.54	10.43	217
12	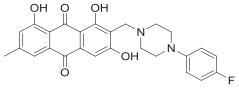	10.44	5.027	23.42
13	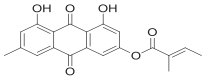	216	35.95	570
14	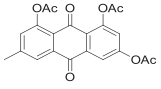	200	2.142	26.47
15	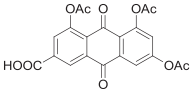	218	8.103	245
III	Epirubicin (marketed drug)	4.6	7.7	3.2

line to its parent compound **1** and C-alkylated derivative **12** found to be 11-fold more potent in HepG2 cell line and 58-fold more potent in MDA-MB-231 cell lines to its parent compound **1**. It is noteworthy to mention here that **3** and **12** showed comparable in vitro anticancer activity with marketed drug epirubicin **III** (Fig. 1 and Table 1), therefore **3** and **12** were selected for cell cycle arrest, caspase dependent apoptosis and DNA binding interaction studies.

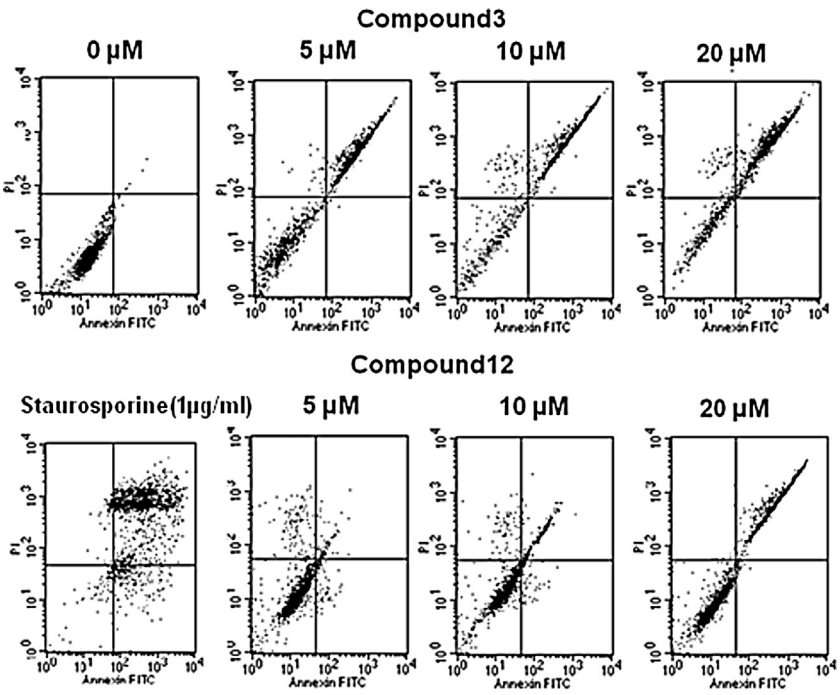

Fig. 5. Determination of apoptosis inducing ability of **3** and **12** by flow cytometry: HepG2 cells (5 × 105 cells) with 70–80% confluence were incubated in RPMI supplemented with 10% FBS without (control) and staurosporine (1 µg/ml) as positive control with 5, 10 and 20 µM of derivatives **3** and **12**. After 24 h, the cells were harvested, stained with Annexin-V-FITC and PI, and analyzed by flow cytometry.

Apoptosis inducing ability studies by flow cytometry

In order to characterize the cellular basis of antiproliferative effects of selected derivatives **3** and **12**, we initially investigated the apoptosis inducing ability by flow cytometry in HepG2 cells (Muktapuram et al. 2012). Annexin-V specially binds to phosphatidylserine and has been employed for determination of apoptotic cells. Annexin-V/PI staining was performed to determine early, late apoptotic and necrotic cells followed by treatment with 5, 10 and 20 µM concentration of derivatives **3** and **12** and staurosporine (1 µg/ml) as positive control in HepG2 cells. When HepG2 cells were stained with annexin-V/PI and analyzed with flow cytometer, early and late apoptosis (annexin V-stained) cells were found to be increased in a dose-dependent manner (Fig. 5), which indicates the induction of apoptosis by **3** and **12**.

Cell cycle arrest studies

To determine the possible effect of these compounds on cell cycle progression, HepG2 cells were treated with 5, 10 and 20 µM

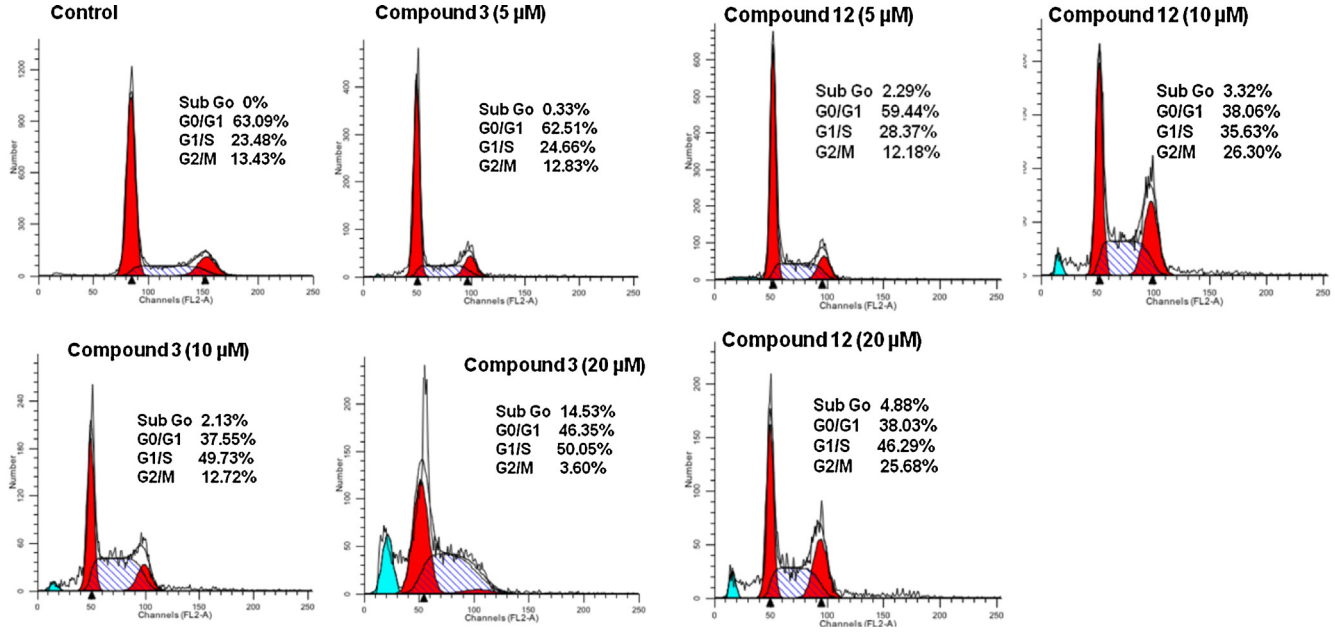

Fig. 6. Effect of derivatives **3** and **12** treatment to HepG2 cells on cell cycle distribution. The cells treated with derivatives **3** and **12** for 24 h were collected and stained with PI and analyzed by flow cytometry. Following FACS analysis, cellular DNA histograms were further analyzed by Modfit LT V3.2.1. The data are representative examples for duplicate tests. The details are described in supporting information.

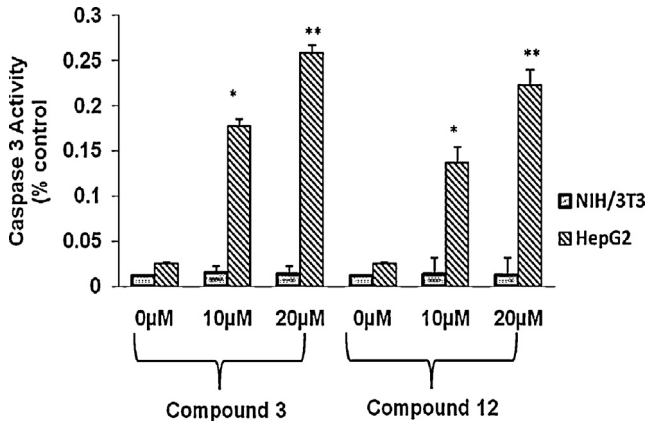

Fig. 7. Effect of **3** and **12** on caspase-3 activity in HepG2 cells and NIH/3T3 cells. After 24 h treatment with or without derivatives **3** and **12**, caspase-3 activities were determined by mixing the cell lysates with colorimetric substrate (Ac-DEVD-pNA). The absorbance was measured at 405 nm in an ELISA reader. Caspase-3 activity was expressed as the change of the activity compared to the control. $^{*}P < 0.05$ and $^{**}P < 0.01$ vs control.

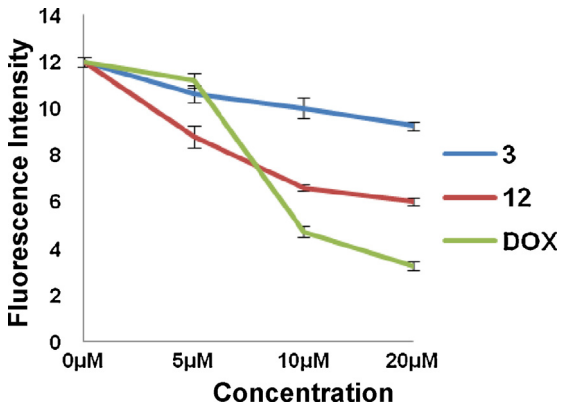

Fig. 8. DNA interacting ability of antiproliferative emodin derivatives **3**, **12** and doxorubicin (**II**); error bars represent the standard deviation of the mean, $n = 3$.

of **3** and **12** then stained with propidium iodide (Fig. 6). To evaluate the distribution of actively dividing cells in the cell cycle before the induction of extensive apoptosis, cells were treated for 24 h, and the percentage of apoptotic and nonapoptotic cells in each phase of the cell cycle was determined by DNA flow cytometry (Sinha et al. 2011). As shown in Fig. 6 cells in the G1/S phase increased from 23.48% in controls to 24.66%, 49.73%, and 50.05% after treatment with **3** and cells in the G1/S phase increased from 23.48% in controls to 28.37%, 35.63%, and 46.29%, after treatment with derivative **12**, indicating that derivatives **3** and **12** arrest cell cycle at G1/S phase. Along with G1/S phase arrest, the sub-G0 population was slightly increased in cells exposed to 10 and 20 μM of **3** and **12**. The results obtained in cell proliferation studies, and apoptosis induction assay also correlates the compound **3** and **12** effects on cell cycle progression.

Caspase-3 activity in HepG2 cells

To find out whether the induction of apoptosis by **3** and **12** via caspase mediated or not, we examined the caspase-3 activation in HepG2 cells and NIH/3T3 cells. Caspases belongs to cysteine proteases class, are the important proteins that regulate the apoptotic response (Fig. 7). Among these, caspase-3 is a key protein in the apoptosis mechanism since it executes both extrinsic and intrinsic pathways (Kamal et al. 2011; Wang et al. 2007). Our studies indicated that a concentration dependent increase in caspase-3 activity with derivatives **3** and **12** treatment as compared with the untreated control. Caspase-3 activation was enhanced 6.88 and 10.03-folds by **3** and 5.33and 8.66-folds by **12** in cells treated with 10 and 20 μM respectively, when compared with control group (Fig. 7) while in normal cells (NIH/3T3) there is no induction of caspase-3 activity. These results confirmed that the apoptosis induction is due to caspase-3 activation by **3** and **12** in HepG2 cells.

DNA binding interaction

In this study we evaluated the DNA interacting ability of antiproliferative emodin derivatives **3** and **12**, using an ethidium bromide displacement assay (Fig. 8). The fluorescence intensity of ethidium bromide increases upon binding of DNA and subsequent displacement of ethidium is apparent by a decrease in emission intensity upon addition of competitive inhibitor (Bair et al. 2010; Dai et al. 2012). We have included doxorubicin **II** (Fig. 1), a known DNA interacting anticancer drug for comparison. Calf thymus DNA was preincubated with ethidium bromide for 30 min in buffer before newly synthesized compound addition. Derivatives **3** and **12** were incubated with ethidium bromide DNA complex for 30 min and measured fluorescence. As shown in Fig. 8, the derivatives **3** and **12** have good DNA binding interaction similar to Doxorubicin (**II**). The compound **12** has better DNA interaction than **3**. These results suggested that potent antiproliferative effect of the derivative **3** and **12** might be due to DNA intercalation.

Conclusions

In conclusion we have isolated large quantities of emodin (**1**) from the roots of *R. emodi* and prepared novel derivatives **2**–**15** and evaluated their in vitro anticancer activity in HepG2 and MDA-MB-231 cell lines. Some of the derivatives showed better therapeutic effect than the parent compound. Among these derivatives **3** and **12** showed comparable in vitro anticancer activity to that of the marketed drug epirubicin (**III**). The Compounds **3** and **12** were capable of inducing cell cycle arrest and caspase dependent apoptosis in HepG2 cell lines and exhibit DNA intercalating activity. These emodin derivatives hold a promise for developing safer alternatives to the marketed Eupirubicin. Further work is progress in our laboratory to evaluate their in vivo anticancer potential and in-depth mechanistic aspects.

Conflict of interest

The authors have no conflict of interest.

Disclosure statement

The authors have nothing to disclose.

Acknowledgments

Authors are thankful to Dr. T.K. Chakraborty, Director, CSIR-CDRI for constant encouragement for the program on natural products of biological importance. We also thank the Ministry of Earth Sciences (MoES) and EMPOWER project from CSIR, New Delhi for providing research grant and fellowship. Komal Sharma is thankful to DST for INSPIRE fellowship. Mr. J.P. Chaturvedi, Miss. Astha Shukla and Miss. Manali Agrawal for technical support, SAIF, CDRI for spectral data.

Appendix A. Supplementary data

Supplementary data associated with this article can be found, in the online version, at http://dx.doi.org/10.1016/j.phymed.2013.03.015.

References

Agarwal, S.K., Singh, S.S., Verma, S., Kumar, S., 2000. Antifungal activity of anthraquinone derivatives from *Rheum emodi*. Journal of Ethnopharmacology 72, 43–46.

Alves, D.S., Perez, F.L., Estepa, A., Micol, V., 2004. Membrane-related effects underlying the biological activity of the anthraquinones emodin and barbaloin. Biochemical Pharmacology 68, 549.

Bair, J.S., Palchaudhuri, R., Hergenrother, P.J., 2010. Chemistry and biology of deoxynyboquinone, a potent inducer of cancer cell death. Journal of the American Chemical Society 132, 5469–5478.

Blicke, F.F., 1942. Mannich reaction. In: Adams, R. (Ed.), Organic Reaction, vol. 1. Wiley, New York, p. 303.

Brewster, J.H., Eliel, E.L., 1953. Carbon–carbon alkylation of amines and ammonium salts. In: Adams, R. (Ed.), Organic Reactions. John Wiley and sons, New York, p. 8.

Chen, R.S., Jhan, J.Y., Su, Y.J., Lee, W.T., Cheng, C.M., Ciou, S.C., Lin, S.T., Chuang, S.M., Ko, J.C., Lin, Y.W., 2009. Emodin enhances gefitinib-induced cytotoxicity via Rad51 down regulation and ERK1/2 inactivation. Experimental Cell Research 315, 2658–2672.

Chen, Y.C., Shen, S.C., Lee, W.R., Hsu, F.L., Lin, H.Y., Ko, C.H., Tseng, S.W., 2002. Emodin induces apoptosis in human promyeloleukemic HL-60 cells accompanied by activation of caspase 3 cascade but independent of reactive oxygen species production. Biochemical Pharmacology 64, 1713–1724.

Chun, G.W., Jun, Q.Y., Bei, Z.L., Dan, T.J., Chong, W., Liang, Z., Dan, Z., Yan, W., 2010. Anti-tumor activity of emodin against human chronic myelocytic leukemia K562 cell lines in vitro and in vivo. European Journal of Pharmacology 627, 33–41.

Dai, X.Y., Zeng, X.X., Peng, F., Han, Y.Y., Lin, H.J., Xu, Y.Z., Zhou, T., Xie, G., Deng, Y., Mao, Y.Q., Yu, L.T., Yang, L., Zhao, Y.L., 2012. A novel anticancer agent. SKLB70359, inhibits human hepatic carcinoma cells proliferation via G0/G1 cell cycle arrest and apoptosis induction. Cellular Physiology and Biochemistry 29, 281–290.

Fain, V.Ya., 1999. 9,10-Anthraquinones and their Use. USSR Academy of sciences, Moscow (in Russian).

Gorelik, M.V., 1983. Chemistry of Anthraquinone and Its Derivatives. USSR Academy of sciences, Moscow (in Russian).

Huang, H.C., Chu, S.H., Chao, P.D., 1991. Vasorelaxants from Chinese herbs, emodin and scoparone, possess immunosuppressive properties. European Journal of Pharmacology 198, 211–213.

Kamal, A., Suresh, P., Mallareddy, A., Kumar, B.A., Reddy, P.V., Rajua, P., Tamboli, J.R., Shaik, T.B., Jain, N., Kalivendi, S.V., 2011. Synthesis of a new 4-aza-2, 3-didehydropodophyllotoxin analogues as potent cytotoxic and antimitotic agents. Bioorganic and Medicinal Chemistry 19, 2349–2358.

Kemertelidze, E.P., Gotsiridze, A.V., 1971a. Khimiya Prirodnykh Soedinenii, 519.

Kemertelidze, E.P., Gotsiridze, A.V., 1971b. Soobshcheniya Akademii Nauk Gruzii. SSR 61, 93.

Kintsurashvili, L.A., Sikharulidze, M.I., Buyanov, V.N., Turabelidze, D.G., 1999. Synthesis of amino derivatives of 1,6 8-trihydroxy-3-methyl-9,10-anthraquinone. Chemistry of Natural Compounds 35, 6.

Koyama, M., Kelly, T.R., Watanabe, K.A., 1988. Novel type of potential anticancer agents derived from chrysophanol and emodin. Some structure–activity relationship studies. Journal of Medicinal Chemistry 31, 283–284.

Kuo, Y.C., Meng, H.C., Tsai, W.J., 2001. Regulation of cell proliferation, inflammatory cytokine production and calcium mobilization in primary human T lymphocytes by emodin from *Polygonum hypoleucum* Ohwi. Inflammation Research 50, 73–82.

Liang, J.W., Hsiu, S.L., Huang, H.C., Lee-Chao, P.D., 1993. HPLC analysis of emodin in serum, herbs and Chinese herbal prescriptions. Journal of Food and Drug Analysis 1, 251–257.

Muktapuram, P.R., Gara, R.K., Sharma, K., Rohit, C., Srinivas, K., Mishra, D.P., Bathula, S.R., 2012. Anticancer siRNA delivery by new anticancer molecule: a novel combination strategy for cancer cell killing. European Journal of Medicinal Chemistry 56, 400–408.

Rahimipour, S., Bilkis, I., Péron, V., Gescheidt, G., Barbosa, F., Mazur, Y., Koch, Y., Weiner, L., Fridkin, M., 2001. Generation of free radicals by emodic acid and its [D-Lys^6]GnRH-conjugate. Photochemistry and Photobiology. 74, 226–236.

Shieh, D.E., Chen, Y.Y., Yen, M.H., Chiang, L.C., Lin, C.C., 2004. Emodin-induced apoptosis through p53-dependent pathway in human hepatoma cells. Life Sciences 74, 2279–2290.

Singh, S.S., Pandey, C.S., Singh, R., Agarwal, K.S., 2005. 1,8-Dihydroxyanthraquinone derivatives from rhizomes of *Rheum emodi*. Indian Journal of Chemistry 43B, 1494–1496.

Sinha, S., Roy, S., Reddy, B.S., Pal, K., Sudhakar, G., Iyer, S., Dutta, S., Wang, E., Vohra, P.K., Roy, K.R., Reddanna, P., Mukhopadhyay, D., Banerjee, R., 2011. Molecular Cancer Research 9, 364.

Su, Y.T., Chang, H.L., Shyue, S.K., Hsu, S.L., 2005. Emodin induces apoptosis in human lung adenocarcinoma cells through a reactive oxygen species-dependent mitochondrial signaling pathway. Biochemical Pharmacology 70, 229–241.

Wang, C., Wu, X., Chen, M., Duan, W., Sun, L., Yan, M., Zhang, L., 2007. Emodin induces apoptosis through caspase 3-dependent pathway in HK-2 cells. Toxicology 231, 120–128.

Yang, F., Zhang, T., Tian, G., Cao, H., Liu, Q., Ito, Y., 1999. Preparative isolation and purification of hydroxyanthraquinones from *Rheum officinale* Baill by high-speed counter-current chromatography using pH-modulated stepwise elution. Journal of Chromatography A 858, 103–107.

Zaprometnov, M.N., 1993. Phenolic Compounds. Distribution, Metabolism, and Functions in Plants. USSR Academy of sciences (Nauka), Moscow (in Russian).

Zhang, L., Lau, Y.K., Kim, R.L.D.S., Chen, C.F., Hortobagyi, G.N., Chang, C., Hung, M.C., 1998. Tyrosine kinase inhibitors, emodin and its derivative repress HER-2/neu-induced cellular transformation and metastasis-associated properties. Oncogene 16, 2855–2863.

Zhang, L., Lau, Y.K., Xia, W., Hortobagyi, G.N., Hung, M.C., 1999. Tyrosine kinase inhibitor emodin suppresses growth of HER-2/neu-over expressing breast cancer cells in athymic mice and sensitizes these cells to the inhibitory effect of paclitaxel. Clinical Cancer Research 5, 343–353.

Zhou, X.M., Chen, Q.H., 1998. Biochemical study of Chinese rhubarb. XXII. Inhibitory effect of anthraquinone derivatives on Na^+-K^+-ATPase of the rabbit renal medulla and their diuretic action. Acta Pharmaceutica Sinica 23, 17–20.